WORLD CONFERENCE ON TIMBER ENGINEERING 2025
BRISBANE, AUSTRALIA
Advancing Timber for the Future Built Environment

QUANTITATIVE EVALUATION OF THE MECHANISM OF ADHESIVE-INDUCED LOAD INCREASE IN PLYWOOD AND LVL UNDER FULL AND PARTIAL COMPRESSIVE STRESS

Ryutaro SUDO[1], Kohta MIYAMOTO[2], Hirofumi IDO[3]

ABSTRACT: The partial compressive performances of adhesively layered wood-based materials are affected by their adhesive layers. Two mechanisms were assumed in this study. Mechanism I attributed to the simple compressive resistance of the adhesively impregnated wood and adhesive layers and Mechanism II attributed to the deformative constraint from adjacent layers when the fiber direction of the layer was perpendicular to that of the adjacent layer (owing to deformation differences). Plywood and LVL were used in this study. A compressive test was conducted with additional length, adhesive, adhesive type, layer composition, and wood species as parameters. Mechanisms I and II are quantitatively evaluated. Mechanism I varied according to the wood species and fiber direction. Mechanism II varied according to the height of the specimen and wood species.

KEYWORDS: plywood (PW), laminated veneer lumber (LVL), partial compression perpendicular to the grain (PCPG), adhesive layer, effect of additional length

1 – INTRODUCTION

Wood-based materials with large cross-sections, such as mass plywood panels and cross-laminated timber (CLT), have recently been developed. These materials are expected to be used in structural applications; however, their mechanical properties must be investigated. The partial compressive performance is an important mechanical property. Researchers [1][2] have reported the contribution of adhesive layers to the partial compressive performance of adhesively layered materials (e.g. plywood (PW), laminated veneer lumber (LVL), and CLT). However, the quantitative effects and mechanisms underlying the contributions of the adhesive layer have not been elucidated. In this study, the mechanisms are classified into two types, and the contributions of these mechanisms are quantitatively evaluated.

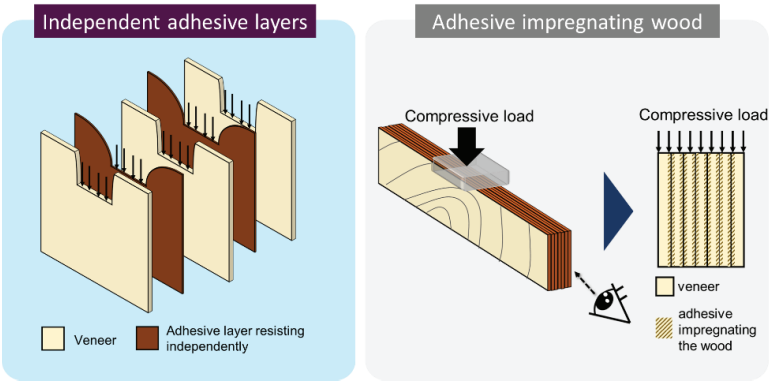

Figure 1. Schematic summarizing Mechanism I.

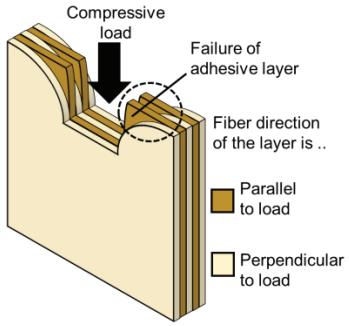

Figure.2. Schematic summarizing Mechanism II.

[1] Ryutaro SUDO, Graduate School of Environmental, Life, Natural Science and Technology, Okayama University, Okayama, Japan, sudoryutaro@okayama-u.ac.jp, ORCID: 0000-0001-6173-695X

[2]Kohta MIYAMOTO, Forestry and Forest Products Research Institute, Tsukuba, Japan, mkohta@ffpri.affrc.go.jp, ORCID: 0009-0003-7059-6196

[3]Hirofumi IDO, Forestry and Forest Products Research Institute, Tsukuba, Japan, ido@ffpri.affrc.go.jp, ORCID: 0000-0002-6787-615X

https://doi.org/10.52202/080513-0199

Mechanism I: Adhesives impregnate the wood and adhesive layers themselves directly resist compressive stress, as shown in Fig. 1. This mechanism seems to be related to the fact that the density of LVL is typically higher than that of timber. The effects of the adhesive layer or adhesive impregnated with wood are expected to vary or be equal depending on the difference in the loading conditions (e.g., with or without any additional length), whereas the fiber direction may or may not influence the effectiveness of the adhesive-impregnated veneer or independent adhesive layer, respectively. If the adhesive layers resisting compressive stress independent of the veneers play the main role in Mechanism I, then Mechanism I is expected to be affected by the loading condition and not by the fiber direction of the veneers.

Mechanism II: Deformation under a partial compressive load varies as a function of the fiber direction, as shown in Fig. 2. When the PW or CLT is partially compressed, the effects of the adjacent layers (constraining each other's deformation) are expected to improve mechanical performance. This effect is not expected to be induced when the materials are exposed to a full compressive load.

This study investigated PW and LVL composed of thin layers. Thus, the effect of the adhesive is expected to be considerable. Full and partial compressive tests were conducted with the existence of additional length, existence of adhesive, adhesive type, layer composition, and wood species as parameters. Mechanisms I and II are quantitatively evaluated.

2 – MATERIALS AND METHOD

Veneers of Japanese cedar (*Cryptomeria japonica*) (referred to as "JC") and Japanese larch (*Larix kaempferi*) (referred to as "JL") (average thickness = 3.9 mm) with dimensions of 310 mm × 310 mm were used as raw materials. The original veneers were divided into groups of seven to ensure that the total densities of all veneer pairs within the same species were approximately equal. PW and LVL were composed of seven layers. These materials were manufactured by performing the following operations: after veneers were dried at 105 ℃ for 24 h, phenol-formaldehyde (PF) or urea-formaldehyde (UF) resin adhesives were manually applied to each veneer layer at a specified spreading rate. The assembled veneer layups were cold- and hot-pressed at specific pressures, pressing times, and temperatures. The

Table 1. Conditions for adhesive operation.

Adhesive type	Spreading rate (g/m^2)	Cold-pressing		Hot-pressing		
		Pressure (MPa)	Pressing time (minute)	Pressure (MPa)	Pressing time (minute)	Temperature (°C)
PF	360-410	1.0	30	0.8	14	130
UF	320-370	1.0	30	0.8	14	110

Table 2. List of specifications.

(i) Verification for Mechanism I.

Shape	Adhesive type	Layer composition	Wood species	Density (kg/m^3)		Thickness (mm)		Moisture content (%)		
				Ave.	S. D.	Ave.	S. D.	Ave.	S. D.	
A	PF	S7	JC	428	9.2	25.5	0.2	7.1	0.1	**
		S0		425	8.6	25.5	0.2	7.2	0.1	**
B		S7		421	8.0	25.6	0.2	7.1	0.1	**
		S0		423	14.5	25.4	0.1	7.2	0.1	**
C		S7		419	9.4	25.6	0.2	7.1	0.1	**
		S0		425	20.4	25.5	0.2	7.2	0.1	**
A	UF	S7		410	8.3	26.1	0.1	10.4	0.4	
		S0		408	10.3	26.2	0.1	10.8	0.4	
B		S7		404	8.4	26.1	0.2	10.4	0.4	
		S0		410	12.2	26.3	0.1	10.8	0.4	
C		S7		395	17.7	26.1	0.1	10.4	0.4	
		S0		409	6.4	26.2	0.2	10.8	0.4	
A	N*	S7		327	4.3	27.8	0.3	5.0	0.1	
		S0		318	5.0	28.0	0.2	4.9	0.1	
B		S7		331	5.0	27.7	0.3	-	-	
		S0		323	8.7	27.7	0.2	-	-	
C		S7		321	11.9	27.8	0.3	-	-	
		S0		312	10.2	27.8	0.2	-	-	
A	PF	S7	JL	627	13.9	26.8	0.2	10.0	0.5	**
		S0		624	13.6	26.6	0.1	9.7	0.3	**
B		S7		622	16.5	26.9	0.2	10.0	0.5	**
		S0		610	13.4	26.6	0.1	9.7	0.3	**
C		S7		613	14.4	26.9	0.2	10.0	0.5	**
		S0		620	7.7	26.6	0.1	9.7	0.3	**
A	N*	S7		530	13.1	28.6	0.3	9.0	1.0	
		S0		524	11.5	28.8	0.2	9.0	0.2	
B		S7		525	11.3	28.6	0.3	-	-	
		S0		527	10.0	28.6	0.3	-	-	
C		S7		521	13.7	28.5	0.4	-	-	
		S0		515	22.2	28.1	0.3	-	-	

(ii) Verification for Mechanism II.

Wood species	Adhesive type	Dimension	Layer composition	Density (kg/m^3)		Thickness (mm)		Moisture content (%)		
				Ave.	S. D.	Ave.	S. D.	Ave.	S. D.	
JC	PF	A	S0	425	8.6	25.5	0.2	7.2	0.1	**
			S1	421	9.0	25.8	0.1	7.2	0.1	
			S3	409	9.5	25.5	0.2	7.1	0.1	
			S7	428	9.2	25.6	0.3	7.1	0.1	**
		B	S0	423	14.5	25.6	0.2	7.2	0.1	**
			S1	423	11.2	25.8	0.1	7.2	0.1	
			S3	408	9.5	25.4	0.1	7.1	0.1	
			S7	421	8.0	25.5	0.1	7.1	0.1	**
		C	S0	425	20.4	25.6	0.2	7.2	0.1	**
			S1	408	16.9	25.9	0.1	7.2	0.1	
			S3	402	16.4	25.5	0.2	7.1	0.1	
			S7	419	9.4	25.7	0.2	7.1	0.1	**
JL	PF	A	S0	624	13.6	26.8	0.2	9.7	0.3	**
			S1	625	12.9	26.8	0.2	9.6	0.5	
			S3	623	18.9	26.6	0.1	9.5	0.5	
			S7	627	13.9	26.7	0.2	10.0	0.5	**
		B	S0	610	13.4	26.9	0.2	9.7	0.3	**
			S1	624	19.9	27.1	0.1	9.6	0.5	
			S3	615	15.9	26.6	0.1	9.5	0.5	
			S7	622	16.5	26.6	0.1	10.0	0.5	**
		C	S0	620	7.7	26.9	0.2	9.7	0.3	**
			S1	605	18.0	27.0	0.1	9.6	0.5	
			S3	624	13.4	26.6	0.1	9.5	0.5	
			S7	613	14.4	26.6	0.2	10.0	0.5	**

*Note; "Ave." means "average", "S. D." means "standard deviation". "-"indicates that the measurement could not be conducted. "N" indicates specifications without adhesives. The symbol ** inidicates specifications shared by the verifications for Mechanisms I and II.*

https://doi.org/10.52202/080513-0199

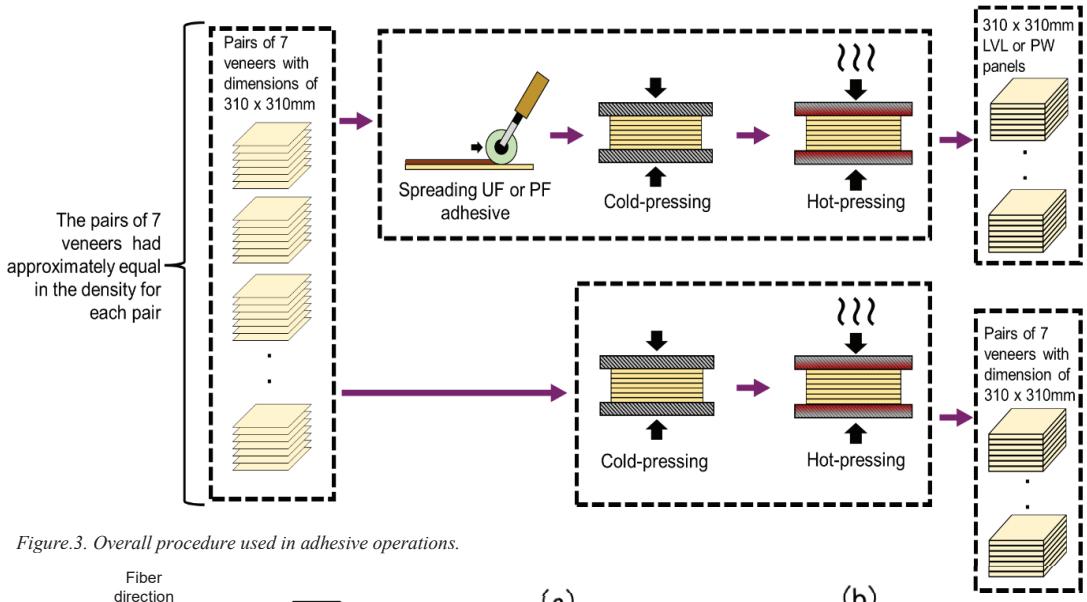

Figure.3. Overall procedure used in adhesive operations.

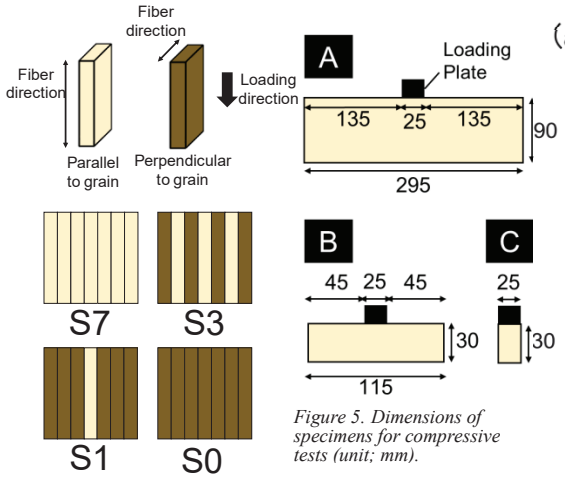

Figure 4. Types of layer compositions.

Figure 5. Dimensions of specimens for compressive tests (unit; mm).

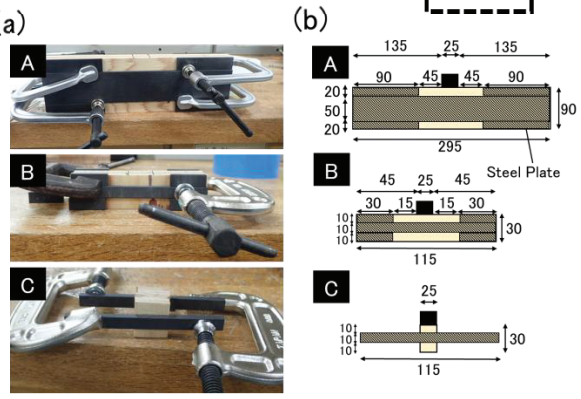

Figure 6. Setup of supporting plate.
Note: (a) Photographs of setup, and (b) dimensions (unit: mm).

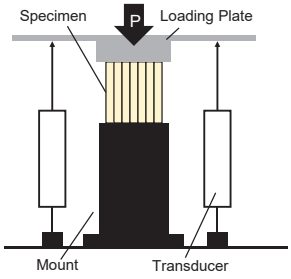

Figure 7. Test apparatus.

spreading rate, pressure, pressing time, and temperature are presented in Table 1. The veneers were laminated with the lathe checks facing inward. Only cold- and hot-pressings were applied to the simply layered veneers without an adhesive. Hereafter, specimens without adhesive are referred to as N-type. Four types of layer compositions, described below, were manufactured for the bonded panels. The overall procedure is illustrated in Fig. 3.

Thirty specifications for verifying Mechanism I and 24 specifications for verifying Mechanism II obtained by cutting the manufactured boards are listed in Table 2. The specifications included average thickness, density, and moisture content. Ten specimens were prepared for each specification. Details of the layer composition and dimensions corresponding to the loading conditions are shown in Figs. 4 and 5, respectively. Some specifications were common among the sets of specifications used to verify Mechanisms I and II. Supporting plates were used to prevent buckling in the nonbonded specimens, as shown in Fig. 6. The additional length (equal to 1.5 times the specimen's height) was applied to specimen types A and B. Previous studies [3] confirmed that an additional length (equal to 1.5 times the specimen's height) could be regarded as an infinite additional length. Supporting plates were also used for the bonded-type specimens to equalize the test conditions. Both sides of the

https://doi.org/10.52202/080513-0199

Table 3. List of LDA and LRA.

Dimension type	Adhesive type	Layer composition	Wood Species	With adhesive				Without adhesive				LDA (N/mm/layer)		LRA	
				Strength (MPa)		Characteristic load (kN)		Strength (MPa)		Characteristic load (kN)					
				Ave.	S.D.	Ave.	S.D.	Ave.	S.D.	Ave.	S.D.	Ave.	S.D.	Ave.	S.D.
A	PF	S7	JC	41.56	2.67	26.52	1.78	28.33	3.40	19.70	2.38	45.4	19.8	1.35	0.19
B	PF	S7	JC	43.16	2.91	27.55	1.86	33.08	2.38	22.95	1.72	30.6	16.9	1.20	0.12
C	PF	S7	JC	41.67	1.03	26.67	0.77	27.75	3.05	19.36	2.10	48.7	14.9	1.38	0.16
A	UF	S7	JC	39.54	2.37	25.82	1.51	28.33	3.40	19.70	2.38	40.8	18.8	1.31	0.18
B	UF	S7	JC	37.95	2.69	24.75	1.70	33.08	2.38	22.95	1.72	12.0	16.1	1.08	0.11
C	UF	S7	JC	34.65	2.36	22.64	1.48	27.75	3.05	19.36	2.10	21.9	17.2	1.17	0.15
A	PF	S7	JL	62.32	4.51	41.81	3.08	36.56	3.48	26.09	2.46	104.8	26.3	1.60	0.19
B	PF	S7	JL	58.80	4.55	39.52	3.12	38.45	5.37	27.37	3.60	81.0	31.8	1.44	0.22
C	PF	S7	JL	52.69	3.73	35.39	2.47	35.15	3.38	24.96	2.43	69.5	23.1	1.42	0.17
A	PF	S0	JC	8.96	0.89	5.71	0.55	5.21	0.60	3.64	0.42	13.8	4.6	1.57	0.24
B	PF	S0	JC	7.93	1.24	5.03	0.79	5.23	1.13	3.63	0.78	9.3	7.4	1.38	0.37
C	PF	S0	JC	6.15	0.89	3.92	0.56	3.48	0.24	2.42	0.17	10.0	3.9	1.62	0.26
A	UF	S0	JC	8.05	0.51	5.27	0.33	5.21	0.60	3.64	0.42	10.9	3.5	1.45	0.19
B	UF	S0	JC	7.58	0.91	4.97	0.61	5.23	1.13	3.63	0.78	8.9	6.6	1.37	0.34
C	UF	S0	JC	5.62	0.44	3.69	0.30	3.48	0.24	2.42	0.17	8.5	2.3	1.52	0.16
A	PF	S0	JL	17.51	2.29	11.62	1.51	8.57	1.36	6.18	0.98	36.3	12.0	1.88	0.38
B	PF	S0	JL	15.72	2.02	10.45	1.32	10.41	2.32	7.43	1.63	20.1	14.0	1.41	0.36
C	PF	S0	JL	11.56	0.89	7.70	0.58	5.07	0.66	3.57	0.47	27.5	5.0	2.16	0.33

displacement of the loading plate were measured using two displacement transducers, and the average displacement divided by the height of the specimen was considered the apparent strain. The load was measured using a load cell and the value divided by the pressure area was regarded as the apparent stress. Test speeds were 0.9 mm/min for specimens with heights of 90 mm and 0.3 mm/min for specimens with a height of 30 mm. The test continued until the apparent strain reached 10%. The test setup is shown in Fig. 7.

3 – VERIFICATION FOR MECHANISM I

The maximum stress was considered as the strength if a peak point was observed in the stress–strain curve at the end of the test (10% strain). However, in the case of the S0 specifications with an additional length (wherein the applied load did not decrease during the test), the strength was determined from the intersection of the two lines

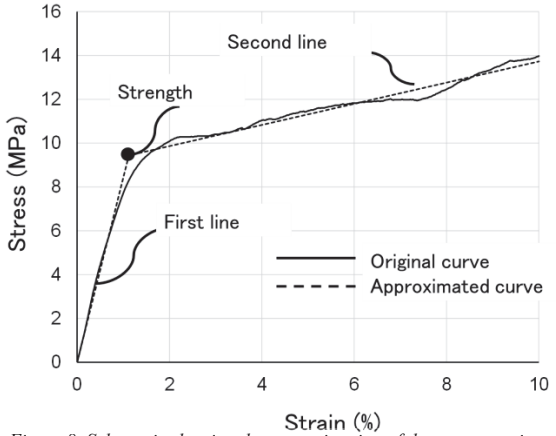

Figure 8. Schematic showing the approximation of the stress–strain curve.

derived by approximating the stress–strain curve, as shown in Fig. 8. The stiffness of the first line was calculated using the 0.1 P_{max} and 0.4 P_{max} points (P_{max} was the maximum stress, inevitably positioned at 10% strain), whereas the intersection and stiffness of the second line were determined by minimizing the sum-of-the-squares of the differences between the original stress–strain curve and the approximated lines.

The strength was multiplied by the pressure area to account for the decrease in thickness during adhesive operation. This value was referred to as the characteristic load. The characteristic load was then divided by the number of adhesive layers (six) and the width of the loading plate (25 mm). The value of the nonbonded type was subtracted from that of the bonded type. These differences were considered load differences with and without the adhesive (LDA). The ratio of the characteristic load between the results with and without the adhesive was also calculated and is referred to as the load ratio with and without the adhesive (LRA). The strength, characteristic load, LDA, and LRA values are presented in Table 3. For example, the average characteristic loads for the specifications with dimension A, adhesive type PF, layer composition S0, and species JC were 5.71 kN with adhesive and 3.64 kN without adhesive. Therefore, LDA was calculated as (5.71 - 3.64) × 1000 / (25 × 6), and yielded the value of 13.8 kN/mm/layer. In addition, the LRA was 5.71 / 3.64 = 1.57. The standard deviations of the LDA and LRA were calculated using the error propagation law.

The LDA and LRA are compared in Fig. 9 (S7 specification) and in Fig. 10 (S0 specification). The LDA

https://doi.org/10.52202/080513-0199

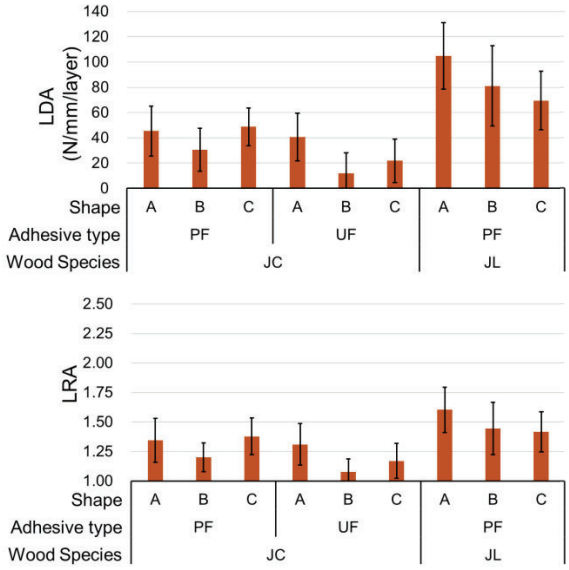

Figure 9. Adhesive effects for specimen with S7 layer composition. Note; Solid and error bars indicate average values and standard deviations, respectively.

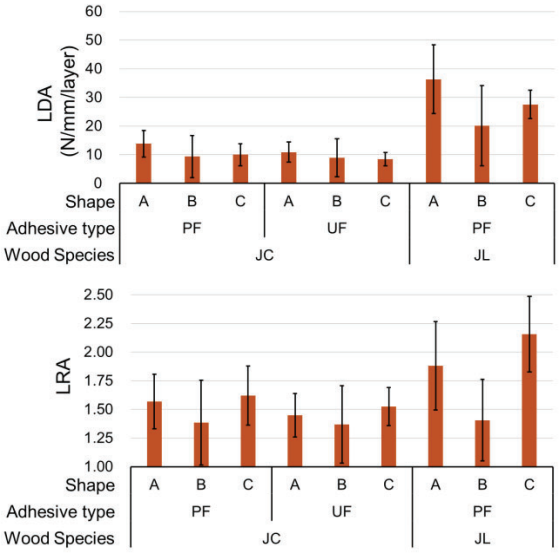

Figure 10. Adhesive effects for specimen with S0 layer composition. Note; Solid and error bars indicate average values and standard deviations, respectively.

for the S7 specification was considerably higher than that for the S0 specification, indicating that the fiber direction had a greater effect and that the independent adhesive layer did not play a major role in the adhesive effect. In addition, no major difference in the LRA was observed between the S7 and S0 specifications; the values were in the ranges of 1.1–1.6 for JC and 1.4–2.2 for JL. The variations in the LDA and LRA with respect to shape, adhesive type, and wood species were minimal. The following discussion focuses on LDA, and its values for the S7 and S0 specifications were examined separately.

The LDA for shape B for the S7 layer composition was lower at JC and higher at JL compared with shape C. Therefore, no consistent trend regarding the additional length was observed. However, the LDA for shape A was higher than those for almost all other shapes, indicating that the specimen height may have had a positive effect on the adhesive effect for the S7 layer composition. To explain this result, we propose a model in which the propagation of cracks along the fiber (causing fractures in the tangential direction) is constrained by the adhesive impregnation of the veneer, as shown in Fig. 11. If the initial crack length did not vary as a function of the specimen's height, an increased specimen height would likely enhance the effectiveness of adhesive impregnation in preventing crack propagation.

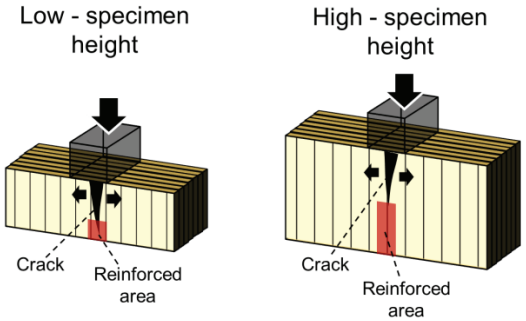

Figure 11. Schematic illustrating adhesive prevention of crack propagation under compressive load parallel to the grain.

Several theoretical studies have been conducted to estimate the partial compressive strength perpendicular to the grain. The improvement in strength due to a sufficient additional length was calculated as follows:

$$f_{pc} = \sqrt{C_{xm}} * f_c \qquad (1-1)$$

$$C_{xm} = 1 + \frac{2}{a}\frac{H}{x_p} \qquad (1-2)$$

where f_{pc} is the partial compressive strength, f_c is the full compressive strength, H is the specimen's height, x_p is the width of the pressure area, and a is a coefficient corresponding to the effect of the additional length.

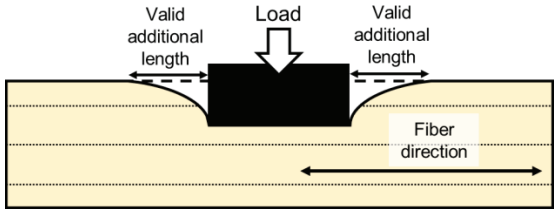

Figure 12. Schematic of valid additional length under partial compressive load perpendicular to the grain.

https://doi.org/10.52202/080513-0199

Table 4. Increasing or decreasing ratios of strength caused by shape differences.

	Wood Species	Adhesive type	B / C		A / B	
			Ave.	S.D.	Ave.	S.D.
Experiment	JC	PF	1.29	0.28	1.13	0.21
		UF	1.35	0.19	1.06	0.14
		N	1.51	0.34	1.00	0.24
	JL	PF	1.36	0.20	1.11	0.20
		N	2.05	0.53	0.82	0.23
Theory		a = 2/3 [5]	2.14	-	1.60	-
		a = 1.5 [3]	1.61	-	1.49	-
		a = 2.5 [4]	1.40	-	1.41	-

Inayama [3] and Kitamori et al. [4] proposed the *a* values of 1.5 and 2.5, respectively. These researchers indicated that the range deforming on the surface in the additional length (referred to as "valid additional length") was concerned with the improvement in the mechanical performance, as shown in Fig. 12, and that the valid additional length was increased proportionally with the specimen's height. The equation proposed by van der Put [5] has a different form from that of equation 1; however, when rearranged, it resembles the original, with a corresponding *a* value of 2/3. The effects of dimensional conditions on the compressive strength perpendicular to the grain are compared in Table 4. The height effect in the N-type was lower than that in the PF and UF types (see columns A/B). These values are lower than the theoretical values. This discrepancy is likely related to the effective depth with respect to the valid additional length, which is suggested to increase with adhesive. The additional length effect in the N-type was greater than that in the PF and UF types (see columns B/C). The N-type values for JC and JL are close to the theoretical values proposed by Inayama [3] and van der Put [4], respectively. However, the specifications with the adhesive were less influenced by the additional length than theoretical estimates, regardless of the wood species.

The LDA for PF was higher than that for UF for both the S7 and S0 layer compositions. When comparing the corresponding specifications of the PF and UF types, the density of the PF was 12–24 kg/m^3 higher than that of the UF, as shown in Table 2. These results suggest that the increase in density owing to the adhesive is related to the improvement in compressive strength. In other words, adhesive impregnating veneer worked effectively.

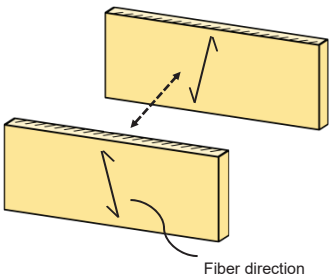

Figure 13. Veneers with SLGs bonded in an in-plane X shape.

The LDA for JL was considerably higher than that for JC with an S7 layer composition. However, the results in Table 2 indicate that the increase in density due to the PF adhesive was in the range of 90–110 kg/m^3 for JC, which was approximately the same as that for JL. This suggests that the increase in compressive strength due to the adhesive is influenced by factors other than density. In other words, the difference in the density derived from the adhesive alone cannot explain the difference in the adhesive effects between JC and JL. We hypothesized that the difference in the slope of the grain (SLG) is a contributing factor. The timber was typically strongest when loaded in the fiber direction, and the strength decreased as load and fiber direction incline. However, strength improved when several veneers with SLGs were bonded in an in-plane X shape, as shown in Fig. 13. If the SLGs were present in the veneers, the angles of the SLGs in all seven veneers were unlikely to be aligned. Therefore, it is likely that the LVL specimen contains one or more cross-banded surfaces, as shown in Fig. 13. This mechanism was more effective at high SLGs because the reinforcement from each layer contributed to its effectiveness. The SLGs of the JC and JL veneers for shape A, adhesive type N, and layer composition S0 were measured because these specifications were the easiest to measure. The average SLGs for JC and JL were 1.3×10^{2} rad and 3.9×10^{2} rad, respectively. Spiral grains, a well-known feature of JL, validated this result. In summary, the higher SLG content of JL compared with that of JC likely contributed to the greater differences between the PF and N types in the JL case compared with those in the JC case.

The LDA for JL was also considerably higher than that for JC with an S0 layer composition. Because SLGs positively affect the strength perpendicular to the grain, unlike that parallel to the grain, the cross-banded surface cannot explain these results. Although the in-plane crossband effect is invalid in the perpendicular

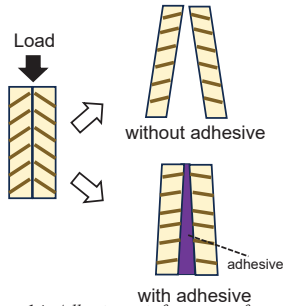

Figure 14. Adhesive reinforcement for veneers with symmetrical AAR.

https://doi.org/10.52202/080513-0199

specification, the out-of-plane crossband effect may have contributed. In other words, the decrease in strength due to the angle of annual rings (AAR) was reinforced by each layer, as shown in Fig. 14. To verify this, the AAR was measured from photographs of the specimens viewed from the side. The targeted specimens had an S7 layer composition, shape A, and adhesive types PF and UF; their cross-sections were sufficiently large for measurements and the sides of the specimens were not excessively fractured. The measured AARs were 1.3×10^{-1} rad for JC and 1.8×10^{-1} rad for JL. Therefore, the out-of-plane crossband effect was greater for JL than for JC. The reinforcement of the defect derived by SLG or AAR was caused by adjacent layers and resembled mechanism II.

4 – VERIFICATION FOR MECHANISM II

The layer compositions of S1 and S3 were calculated based on the experimental data for S0 and S7, respectively. It was assumed (based on calculations) that the performances of S1 and S3 could be determined by adding the performances of all individual layers (i.e., neglecting mechanism II) using equation 2-1, 2,

$$\sigma_{ave\_comp} = \frac{n * \sigma_{ave\_pa} + (7-n) * \sigma_{ave\_pe}}{7} \quad (2-1)$$

$$\sigma_{sd\_comp} = \sqrt{\frac{n * {\sigma_{sd\_pa}}^2 + (7-n) * {\sigma_{sd\_pe}}^2}{7}} \quad (2-2)$$

where σ_{ave_comp} is the calculated stress of the S1 or S3 types at the specific strain, n is 1 for S1 and 3 for S3, σ_{ave_pa} is the average stress of the S7 type at the specific

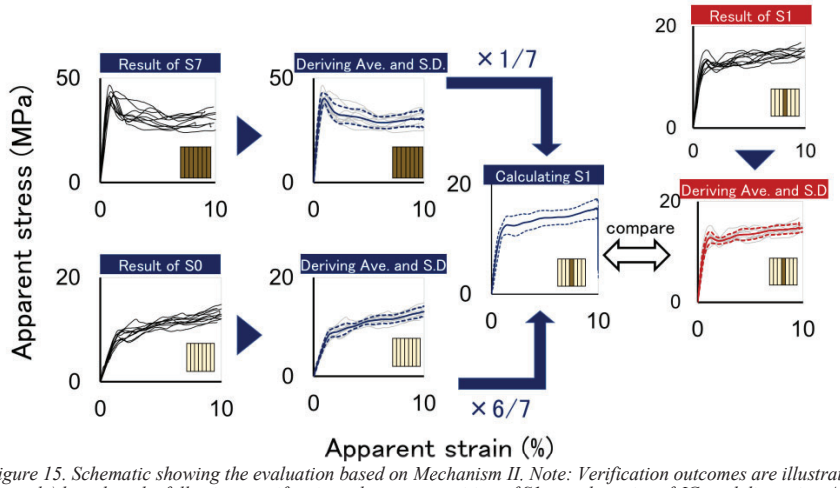

Figure 15. Schematic showing the evaluation based on Mechanism II. Note: Verification outcomes are illustrated (as an example) based on the following specifications: layer composition of S1, wood species of JC, and dimension A.

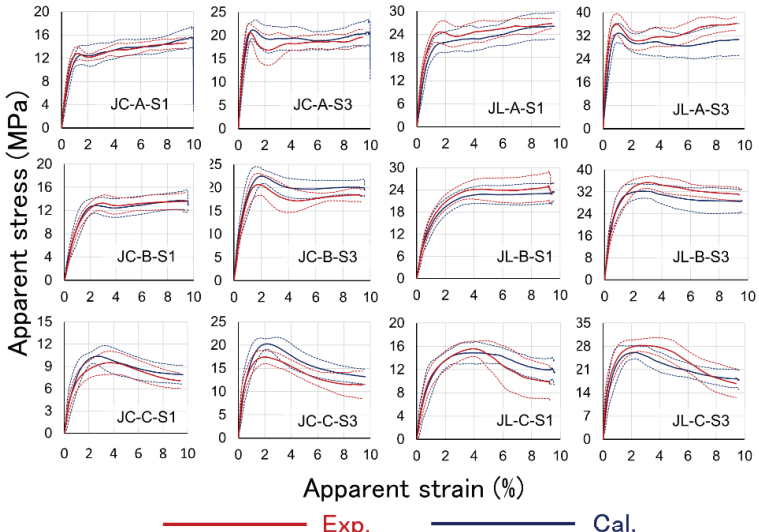

Figure 16. Stress–strain curves. Note: Solid lines show the average, and dotted lines show the average ± standard deviation.

https://doi.org/10.52202/080513-0199

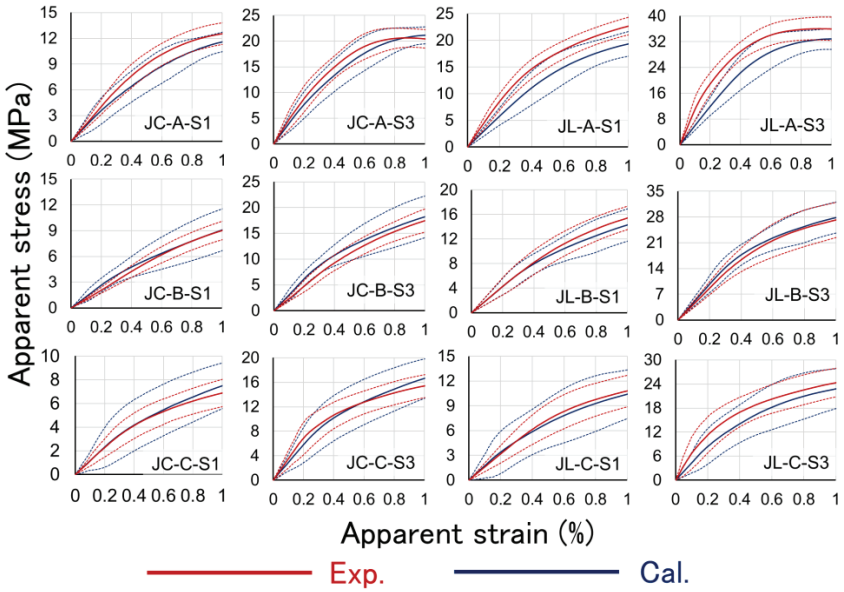

Figure 17. Stress–strain curves under 1% strain. Note: Solid lines show the average, and dotted lines show the average ± standard deviation.

strain, σ_{ave_pe} is the average stress of the S0 type at the specific strain, σ_{sd_comp} is the calculated standard deviation of the stress of the S1 or S3 types at the specific strain, σ_{sd_pa} is the standard deviation of the stress of the S7 type at the specific strain, and σ_{sd_pe} is the standard deviation of the stress of the S0 type at the specific strain.

The calculated and experimental results of the layer compositions of S1 and S3 were compared. A schematic of this procedure is shown in Fig. 15. The overall stress–strain curves and stress–strain curves under 1% strain are shown in Figs. 16 and 17, respectively. For the quantitative evaluation of Mechanism II, the stress at 0.5% strain was regarded as the representative value of the initial stiffness. The values of stress at 0.5% strain are shown in Fig. 18. When the experimental data were higher than the calculated data, Mechanism II was considered valid. A considerable difference was observed in the shape of type A. As the increase of the height of the specimen increases the range of the additional length affected by the loading plate (referred to in previous parts as "valid additional length"), Mechanism II exhibits greater effects on the dimension of A than those on the dimension of B. Because dimension C does not have an additional length, Mechanism II was not observed. Moreover, Mechanism II was more dominant in Japanese larch than in Japanese cedar. For dimension A, the variation in the stress at 0.5% strain by Mechanism II was in the ranges of 10–20% for JC and 20–30%.

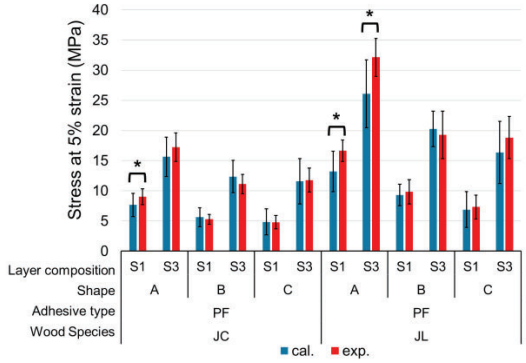

*Figure 18. Comparison of stress at 0.5% strain. * $p < 0.05$.*

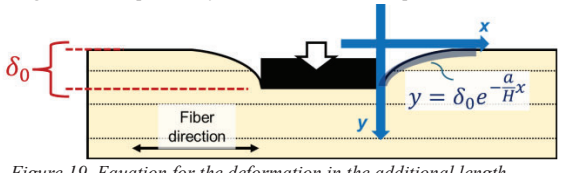

Figure 19. Equation for the deformation in the additional length loaded perpendicular to the grain.

Researchers claimed [3][4] that the deformation on the surface in the additional length obeys an exponential relationship (see Fig. 19). This figure suggests that the deformation is related to the specimen height and the coefficient *a* (referred to in equation 1). Higher specimen height and lower *a* values icreased the valid additional length, as the exponential curve becomes smoother. The deformation is related to an improvement in the apparent stiffness. The apparent elastic modulus with sufficient additional length in the perpendicular direction is calculated as follows:

$$E_{pc} = C_{xm} * E_c \quad (3)$$

where E_{pc} is the apparent elastic modulus under partial compressive load conditions, and E_c is the elastic modulus under full compressive load conditions.The optimal values of *a* (corresponding to each wood species) were calculated using the apparent elastic modulus of the

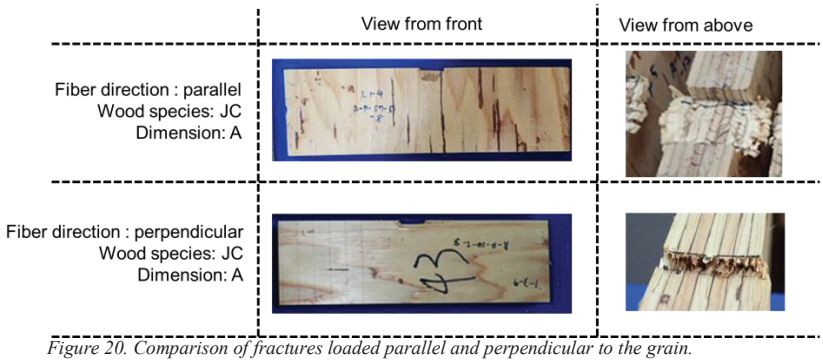

Figure 20. Comparison of fractures loaded parallel and perpendicular to the grain.

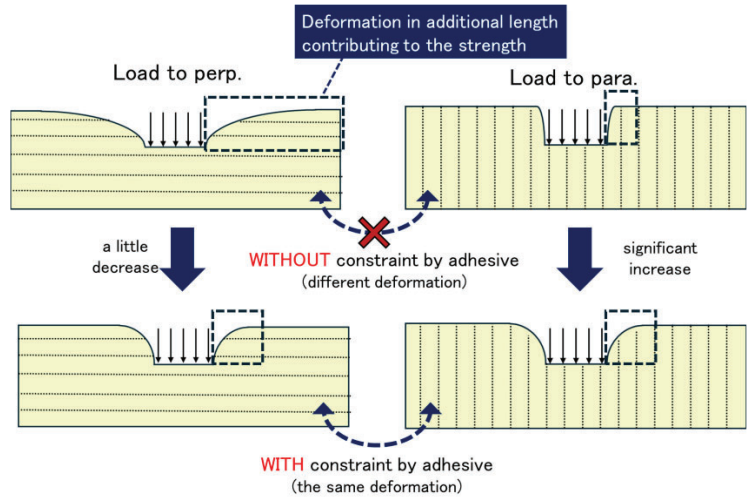

Figure 21. Proposed model regarding Mechanism II.

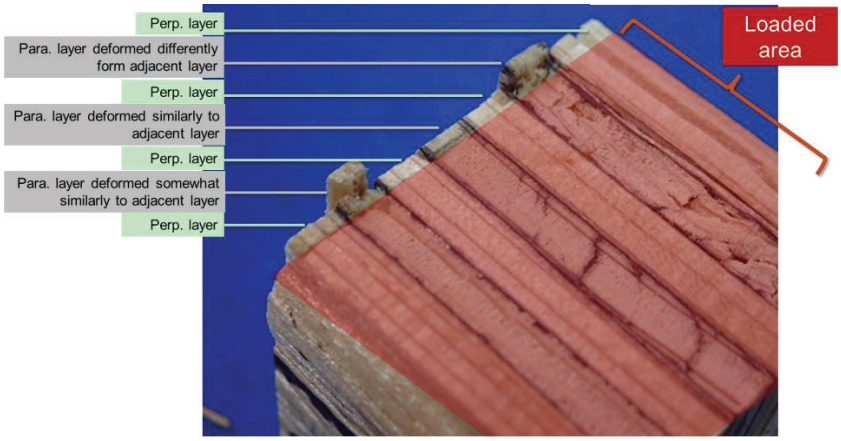

Figure 22. Parallel layers deforming similarly to or differently from the adjacent layer.

S0 type. Equation (1-2) and (3) were used for the calculations: The least-squares method was executed. Consequently, the optimized *a* values were 5.44 for JC and 3.32 for JL. Therefore, Mechanism II was more effective in the case of the specification associated with the greater additional length deformation, exhibiting a smoother exponential curve.

Because the relationship between Mechanism II and the valid additional length was suggested, the following mechanism was hypothesized: The specimen's surface in the additional length was not deformed by the load parallel to the grain but was deformed by the load perpendicular to the grain, as shown in Fig. 20. Assuming that these deformations in the additional length match those in the bonded specimen, the effect of the additional length may be enhanced in the layer parallel to the grain, whereas that perpendicular to the grain may decrease, as depicted in Fig. 21. The former influence may exceed the latter because the performance in the layer parallel to the

https://doi.org/10.52202/080513-0199

grain was much higher than that perpendicular to the grain. This model is overally consistent with the result in the present study.

Fig. 22 shows an illustration of a partially compressed specimen (dimensions C, wood species JL, and layer composition S3) for trial purposes. This specimen was loaded under the elastic limit and then unloaded because deformation was observed before complete fracture. Deformations of some layers parallel and perpendicular to the grain were observed, as in the proposed model.

5 – CONCLUSIONS

Several types of layered wood-based materials exist. Adhesive effects enhancing the mechanical performance of these materials have also been reported. We assumed two types of mechanisms; Mechanism I induced by the adhesive-impregnating veneer and adhesive layer, and Mechanism II induced by constraining deformation by each adjacent orthogonal layer. These two mechanisms were evaluated quantitatively in this study. Mechanism I was evaluated by comparing the test results of the bonded specimen to those of the nonbonded specimen, whereas Mechanism II was evaluated by comparing the test results to the simply calculated results. The main findings of this study are as follows.

Mechanism I was hardly influenced by the presence of the additional length. The specimen's height had a positive effect on Mechanism I for S7 layer composition. The degree of improvement in the mechanical performance under the partial compressive load with the S0 layer composition derived from the presence of the additional length and specimen height was respectively diminished and enhanced by the adhesive. Mechanism I varied according to the adhesive type, which was attributed to variations in density. Mechanism I varied according to the wood species and was attributed to the variations in the SLG and AAR of the original veneer.

Mechanism II was observed only in the cases of specimens with the highest height and sufficient additional length. Mechanism II was more prevalent in the JL group compared with that of the JC group. Theoretical verifications suggested that the valid additional length enhanced Mechanism II. The discussion presented above and the deformation behavior in the test led to a mechanical model in which the deformations of some layers parallel to the grain (in the additional length) matched those perpendicular to the grain (in the additional length).

Quantitative evaluation of the adhesive effect in the LVL and PW was successful in this study. While the difference in the adhesive effect by some parameters (dimensions, adhesive types, and wood species) could be reasonably associated with some properties of the specimen, it was not completely demonstrated owing to the lack of specifications and elemental tests. Furthermore, whether these findings are valid for other layered materials, such as CLT and glued laminated timber, needs to be investigated. However, the findings of this study contribute to a more precise and efficient evaluation of the partial and full compressive strengths of LVL and other laminated wood-based materials with arbitrary layer compositions and adhesive types based on the mechanical properties of the raw layers, such as veneers.

6 – REFERENCES

[1] H Ido, H Nagao, H Kato, A Miyatake, and Y Hiramatsu; "Strength properties of laminated veneer lumber in compression perpendicular to its grain" In Journal of Wood Science 56 (2010), pp. 422–428.

[2] E Tuhkanen, J Molder, and G Schickhofer; "Influence of number of layers on embedment strength of dowel-type connections for glulam and cross-laminated timber" In Engineering Structures 176 (2018), pp. 361–368.

[3] M Inayama, "Study on compression perpendicular to the grain in wood Part 4: Analytic functions for the relation between compression load and elastic deformation perpendicular to the grain in wood" In: Annual Meeting of Architecture Institute of Japan 1993. Tokyo, September 1993. Summaries of Technical Papers of Annual meeting AIJ (1993), pp.907–908.

[4] A Kitamori, T Mori, Y Kataoka, K Komatsu, "Effect of additional length on partial compression perpendicular to the grain of wood: difference among the supporting conditions" In Journal of Structural and Construction Engineering AIJ, 74 (2009), pp.1477–1485.

[5] TACM van der Put, "Derivation of the bearing strength perpendicular to the grain of locally loaded timber blocks" In Holz als Roh- und Werkstoff 66 (2008), pp.409–417.

ACKNOWLEDGEMENT

The adhesive used in this study was supplied by the Oshika Corporation. This study was supported by a Grant-in-Aid for JSPS Research Fellows (No. 23K19311). We are deeply grateful to all of those involved in this study.